Smart Structures and Systems, Vol. 7, No. 1 (2011) 41-57
DOI: http://dx.doi.org/10.12989/sss.2011.7.1.041

Fatigue laboratory tests toward the design of SMA portico-braces

G. Carreras[1], F. Casciati*[2], S. Casciati[3], A. Isalgue[1], A. Marzi[2] and V. Torra[1]

[1]Department of Applied Physics, ETSECCPB, UPC, E-08034 Barcelona, Catalonia, Spain
[2]Department of Structural Mechanics, University of Pavia, Pavia, Italy
[3]Department ASTRA, University of Catania, Syracuse, Italy

(Received January 31, 2010, Accepted October 4, 2010)

Abstract. A deeper understanding of the effectiveness of adopting devices mounting shape memory alloy (SMA) elements in applications targeted to the mitigation of vibrations is pursued via an experimental approach. During a seismic event, less than 1000 loading-unloading cycles of the alloy are required to mitigate the earthquake effects. However, the aging effects during the time of inactivity prior to the oscillations (several decades characterized by the yearly summer-winter temperature wave) should be considered in order to avoid and/or minimize them. In this paper, the results obtained by carrying out, in different laboratories, fatigue tests on SMA specimens are compared and discussed. Furthermore, the effects of seismic events on a steel structure, with and without SMA dampers, are numerically simulated using ANSYS. Under an earthquake excitation, the SMA devices halve the oscillation amplitudes and show re-centering properties. To confirm this result, an experimental campaign is conducted by actually installing the proposed devices on a physical model of the structure and by evaluating their performance under different excitations induced by an actuator.

Keywords: damping; fatigue life; passive control systems; shape memory alloys; vibration mitigation.

1. Introduction

The development of an effective strategy for the mitigation of earthquake induced vibrations must cope with the growing requirements of ameliorating the quality of life. Recently, elements made of shape memory alloy (SMA) were proposed as useful parts of the passive control devices for Civil Engineering applications (see Auricchio *et al*. 2001, Torra *et al.* 2007b, Casciati and Faravelli 2008, Casciati and van der Eijk 2008, Torra *et al*. 2009b, Casciati and Faravelli 2009 and related references).

SMA elements show a hysteretic response to loading-unloading cycles due to their martensitic transformation, also called a first order phase transformation, which is characterized by a locally invariant order of the so-called "military" characteristics, in the sense that the atomic neighbour order is preserved. In the stress induced behavior, the transformation process (from parent to martensite) releases a heat, $Q_{p\rightarrow m}$, corresponding to the macroscopic effect of the latent heat, $l_{p\rightarrow m}$. On the other hand, in the reverse path (from martensite to parent), the heat, $Q_{m\rightarrow p}$, which is related to the latent heat, $l_{m\rightarrow p}$, is absorbed by the alloy. Along the reversed process, the hysteretic work, ${}^{H}W$, which corresponds to the dissipated heat in the hysteresis cycle according to the First Thermodynamics

*Corresponding Author, Professor, E-mail: fabio@dipmec.unipv.it

Law, is given by the sum of the absorbed and released heats

$$^{H}W = Q_{\mathrm{p}\to\mathrm{m}} + Q_{\mathrm{m}\to\mathrm{p}} = \oint f\,dx \tag{1}$$

where the associated force and displacement are denoted by f and x, respectively.

Eq. (1) implies that, in SMA components, the damping effect depends on the absorption of the mechanical work, ^{H}W, which arises, during the loading-unloading cycles, as the net released heat resulting from the balance between the released and absorbed heats in the SMA transformation along the hysteretic cycle. Indeed, a thermodynamic description of the hysteretic cycle establishes that the latent heats are different in the forward and backward transformations, because the released and absorbed heats occur at different stresses. For cycles at constant loads of different values in the forward and backward transformations (as the ones performed, for instance, on NiTi thin wires), it is possible to demonstrate, using the energy balance and the Second Law of Thermodynamics (Isalgue *et al*. 2008), that the difference in the latent heat and the related stress is the origin of the net dissipated energy associated to the hysteretic work, ^{H}W. Note that the latent heat is a function of stress and temperature, in a three coordinates representation of solid materials.

For each application, a careful analysis of its explicit (as well as implicit) requirements is very important in order to achieve the desired behavior of the material. For instance, a macroscopic or mesoscopic property, such as the hysteresis cycle, evolves as the cycling progresses. The origins of this evolution may be associated to plastic deformation and interaction between the interface corresponding to phase transition and the grain boundaries, the precipitates and/or other defects (Lovey and Torra 1999). Furthermore, the atomic diffusion (which sometimes results to either be partially or totally recoverable) modifies the transformation temperatures and may change the hysteresis position due to the Clausius-Clapeyron equation.

In addition, it is necessary to include in the analyses some macroscopic effects, such as self-heating and the specific dependency of the loading-unloading cycles on the frequency. As it occurs in any damper (including both the passive devices, as the ones mounting SMA elements, and the semi-active devices, as the MR dampers), the self-heating of the alloy is an intrinsic aspect of the damping process due to the conversion of work into heat. At very low frequencies, i.e., less than 0.1 Hz, the self-heating effect is negligible, since the time duration is long enough to permit a relevant transmission of heat to the surrounding elements (Torra *et al*. 2009a). Nevertheless, when the SMA elements are demanded to work under values of the oscillation frequencies which can be realistically estimated of the order of 1 Hz or higher during a seismic event, the self-heating effect becomes relevant and the mean value of the SMA temperature might increase several degrees. In this case, the change of temperature can potentially induce a modification of state in the SMA elements and, therefore, the self-heating effect needs to be carefully monitored and analyzed.

Moreover, there is also a spontaneous increase of the length of the sample as the cycling process progresses. The SMA creep must be kept under control in order to ensure an effective damping with the expected length. The balance equation in (1) is only valid when the shape of the hysteresis cycle remains strictly invariant, and this circumstance occurs when the internal state of the material is unchanged. Conversely, changes in the hysteresis cycle indicate the appearance of parasitic effects that modify the internal state of the sample (i.e., its internal energy). These parasitic effects can either be of microscopic nature, such as the atomic order and the creation of dislocations, or macroscopic actions, such as plastic deformations, with or without stabilized martensite, which include, for instance, the increase of the sample length due to the SMA creep (Lovey and Torra 1999).

In this paper, basic concepts from the material science background on SMAs are initially recalled to pave the way toward their possible exploitation in damping the effects of the earthquake actions on a portico. The main content consists of estimating the required properties of a CuAlBe alloy so that a good design, performance and durability of the alloy component can be achieved in terms of an appropriate fatigue life and the stability of the material with time and temperature changes.

In Section 2, the essential requirements of the SMA devices are studied based on the estimates of the minimal stress level and the time and room temperature effects, when the dampers are installed on a structure for several years/decades without undergoing an earthquake. Section 3 is dedicated to experimental fatigue studies on alloy samples of composition CuAlBe; an appropriated thermo-mechanical treatment to improve their performance is also discussed. In Section 4, the dynamic effects of temperature and aging are quantified with reference to the investigated alloy. In Section 5, the application of braces in CuAlBe to the portico of a family house is numerically simulated to evaluate the beneficial effects of SMA dampers in reducing the oscillation amplitudes. Lastly, a physical model of the same portico is used to undergo experimental tests with and without SMA braces.

2. Earthquake applications

In this work, the application of damping devices mounting SMA components (Dunne *et al*. 2004, Johnson *et al*. 2008, Cardone and Dolce 2009) is targeted to mitigate the earthquake induced vibrations in a specific class of structures, including residential buildings and family houses whose structural scheme is essentially made of a framed storey surmounted by a rather rigid floor. To provide an example of a seismic event which mainly damaged this type of structures, reference is made to the earthquake of magnitude 6.9, which occurred on March 25, 2007, in the Ishikawa Prefecture, located near the Noto Peninsula, in the Western side of Honshu Island, in Japan. The epicenter was identified at a depth of 11 km below the ground surface. According to the report from the Fire and Disaster Management Agency issued on April 2, 2007, one person died, 297 were injured, 321 houses collapsed, and other 357 houses were severely damaged. It is worth noting that the damage

Fig. 1 Wajima city located in the north end of Noto Peninsula experienced the largest damage during the March 25, 2007, seismic event. The structure of Miyashita Wood was collapsed but the roof preserved its shape (courtesy of M. Torra)

was limited to old wooden houses, as the one shown in Fig. 1 (ABS Consulting Inc. 2007). The application discussed in Section 5 refers to the same class of buildings with a structural system made of steel.

When focus is placed on the mitigation of seismic effects, four main requirements that a SMA component in a device must satisfy are identified based on the considerations reported in the Introduction:

1) The fatigue-life of the material needs to be, at least, 1000 working cycles. This statement is based on the assumption that the duration of the seismic event is about 1 minute, and that 3 or 4 replicates may occur. With an oscillation frequency of 1 Hz, a satisfactory working behavior of SMA should be observed up to 1000 working cycles.
2) The self-heating effect must be evaluated. Indeed, the heat dissipated by the hysteresis (${}^{H}W$) rises the temperature of the specimen. A typical stress-strain diagram of a CuAlBe alloy under repeated loading-unloading cycles is shown in Fig. 2. The stress value, σ, at which the slope decreases during the loading represents the threshold to be overcome in order to obtain hysteresis along the unloading. As a consequence of the alloy self-heating, an increase of σ is expected due to the Clausius-Clapeyron (CC) thermodynamic equation (Isalgue *et al*. 2008, Aernoudt *et al*. 1989, Wollants *et al*. 1993). The Clausius – Clapeyron equation determines, in the coexistence zone (coex) of the two phases of the material, the position of the hysteresis cycle as the temperature T varies, by evaluating the slope $(\mathrm{d}\sigma/\mathrm{d}T)_{\mathrm{coex}}$ in the stress-strain coordinates. In these coordinates, the CC equation reads

$$(\alpha_{\mathrm{CC}})_{\sigma\text{–}\varepsilon} = (\mathrm{d}\sigma/\mathrm{d}T)_{\mathrm{coex}} = \Delta S_{\mathrm{m}\rightarrow\mathrm{p}}/(\varepsilon V_p) \tag{2}$$

$\Delta S_{\mathrm{m}\rightarrow\mathrm{p}}$ indicates the entropy change in the transformation, and V_p is the parent molar volume. Alternatively, when reference is made to the external force and the associated displacement the Clausius-Clapeyron coefficient, α_{CC}, is written

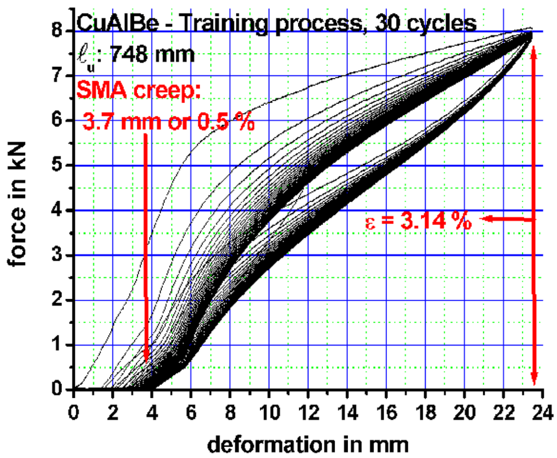

Fig. 2 Effects of training the alloy by applying loading-unloading cycles in traction at room temperature. The specimen of CuAlBe alloy (made of two wires of diameter 3.4 mm and length 748 mm) preliminarily underwent 10 min at 820 C, quench in water at room temperature and aging at 100 C for 1 or 2 months. In this case, the SMA creep is such that deformations greater than 2.5% occur without residual deformation

$$(\alpha_{CC})_{f\text{-}x} = (\mathrm{d}f/\mathrm{d}T)_{\mathrm{coex}} = (V_{\mathrm{p}}\ \Delta h_{\mathrm{m}\rightarrow\mathrm{p}})/(T\ x) \tag{3}$$

where f is the force at which the slope of the diagram decreases, and $\Delta h_{\mathrm{m}\rightarrow\mathrm{p}}$ is the enthalpy change between the martensite and the parent phases, being x the associated length change. The value of the CC coefficient for a CuAlBe alloy was estimated in (Isalgue *et al.* 2006). An instantaneous temperature change of 40 ºC results in a drop of nearly 80 MPa in the σ value.

3) Since the earthquake event is likely to occur after a long time from the damper installation (several years or decades), the atomic diffusion effects in Cu-based alloys need to be avoided or quantitatively determined.
4) It is also required that the action of 10 or more summer-winter cycles of temperature will not dangerously modify the required material properties of the SMA elements.

Items 3 and 4 seem to be coupled, since they are both driven by temperature variations and they both influence the position and the shape of the hysteresis loop in the stress-strain plane. Indeed, the transformation phase temperatures, which are affected by the atomic diffusion effect depending on the internal state of the material, are also sensitive to temperature changes, but their values evolve slowly after sudden external temperature variations which, instead, cause instantaneous drops in the σ value, due to the CC effect.

Focusing on the martensite start transformation temperature, M_{s} its time derivative can modelled by an equation of the type (Isalgue *et al.* 2006)

$$(\mathrm{d}M_{\mathrm{s}}/\mathrm{d}t) = \text{function (material state, } T(t)) \tag{4}$$

where the room temperature T is explicitly regarded as a function of the time t (Fig. 3). While this function is strictly monotonic for a Ni-Ti alloy, it fluctuates up and down for a Cu-based alloy.

Eq. (4) and the relatively slow evolution of M_s provide the theoretical support which justifies the different influences exerted on M_s by the day-night and the winter-summer temperature variations. Indeed, as day-night temperature changes occur, only the Clausius-Clapeyron instantaneous effect on the the σ value applies, while no changes of M_s are observed. The winter-summer temperature variations, instead, actually cause M_s changes, in addition to the CC effect.

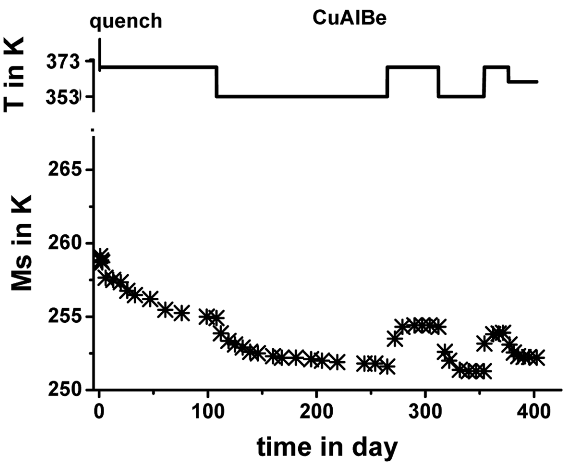

Fig. 3 Evolution in time of the martensite starting temperature, M_s, of a CuAlBe specimen for a given temperature time history; it provides a graphical representation of Eq. (4)

3. Fatigue life of SMA specimens

The results of several experimental campaigns carried out to investigate the fatigue life of SMA samples of different composition were recently published and presented (Casciati *et al*. 2007, 2008, Casciati and Faravelli 2006, Terriault *et al*. 2007, Torra *et al*. 2007a, Casciati and Marzi 2010). Namely, both CuAlBe and NiTi alloys were considered. In the present work, a further understanding of the fatigue behavior of a CuAlBe alloy only is pursued in order to investigate its applicative potential in Civil Engineering. It is worth noting that, in many civil structures, the exposure to harsh chemical conditions is a major concern that could lead to the corrosion of the Cu-based components. Therefore, the target application discussed in Section 5 is conceived with the SMA wires protected inside suitable panels.

The preparation of the "as received" CuAlBe alloy requires some thermo-mechanical treatment. First, a homogenization process is applied and it consists of leaving the alloy for several minutes (less than 10) at a temperature of 1100 K, and then performing an immediate quench in water at room temperature (at about 293 K). After the quench, a suitable aging needs to be implemented. For instance, the alloy can be placed for one or two months at a temperature of 373 K, and then at 353 K for a supplementary aging time. The task of these aging processes is to smooth the residual effects of the homogenization and quenching temperatures in the alloy. In particular, the effects on the values of the transformation temperature, M_s (the so-called "martensite starting temperature"), are smoothed so that these values can clearly track the room temperature changes. A quantitative estimate of the achieved stabilization of the material behavior is provided in Fig. 3. The time effects associated to all summer-winter temperature cycles are also smoothed.

After the aging, experiments based on standard material testing techniques are carried out using an MTS 810 universal servo-hydraulic machine powered by a hydraulic system MTS Silent Flow. Force measurements are acquired by the load cell of an MTS 100 kN actuator. The length of a standard specimen is about equal to 120 mm (while the length of the specimens used in the portico application discussed in Section 5 is, instead, about equal to 800 mm). The plots in Figs. 2 and 4 were obtained during these tests. In Fig. 4, the standard behaviour of a poly-crystalline CuAlBe sample shows a deformation which progressively accumulates with time during a series of cycles of increased amplitude.

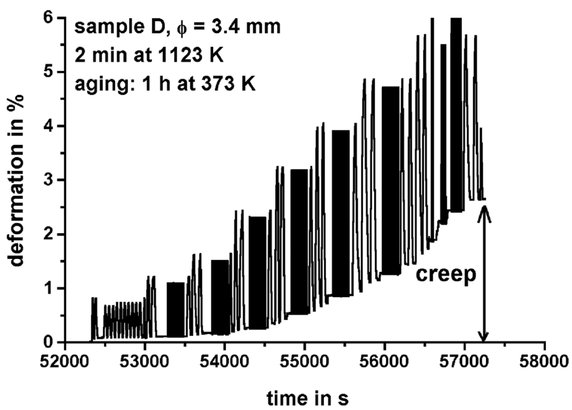

Fig. 4 Standard behaviour of a poly-crystalline CuAlBe sample of length 100 mm: progressive deformation is accumulated with time during a series of cycles of increased amplitude. In practice, the available lengthening is about equal to 3%

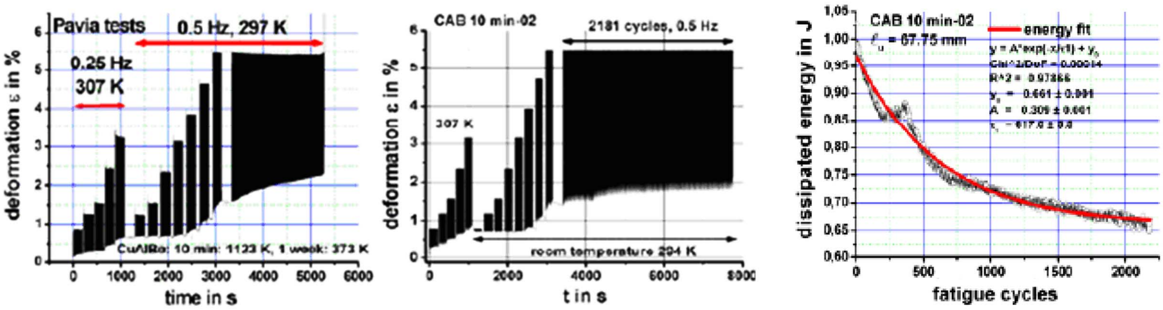

(a) (b) (c)

Fig. 5 Thermo-mechanical tests for fatigue life estimates of a CuAlBe alloy: (a) initial training and more that 1000 working cycles in fatigue of a sample that underwent one week of aging at 373°K (Pavia laboratory), (b) similar experiment but after 1 month at 393°K (Barcelona laboratory) and (c) evolution of the hysteresys energy per cycle with cycling for case (b).

Further tests need to be performed to ensure that the resulting CuAlBe sample shows a satisfactory fatigue life, being able to survive the required number of loading-unloading cycles at a specific temperature and for a given heat treatment of the sample. For this purpose, several thermo-mechanical tests can be conceived. An example is provided by the plots in Fig. 5, where the results from experiments carried out in two different laboratories, one in Pavia, Italy (Fig. 5(a)), and the other in Barcelona, Spain (Figs. 5(b) and 5(c)), are reported. The tests are performed following a similar procedure which includes an initial training of the alloy by a series of progressive cycles performed at a temperature of either 303 or 313 K up to a strain of 3.24%, and a further series of loading-unloading cycles conducted at room temperature (at about 293 K) up to a maximum strain of 5.5%. In the laboratory of Pavia, the test is carried out in span control during the loading and in force control during the unloading in order to avoid compression.

Instead, the Barcelona test is entirely carried out in span control and a special device is utilized to prevent the specimen from undergoing compression. To emphasize the influence of the sample preparation on the actual fatigue behavior of the alloy, samples resulting from ageing processes of different durations (1 week in Pavia and 1 month in Barcelona) are used for the two experiments. As a result, different creep effects are observed. When the thermo-mechanical cycles are applied to a sample aged for one month (Fig. 5(b)), the initial creep approaches a strain of 1.5% and the fatigue cycles increase the creep by 0.3%. A larger increase of the initial creep can be detected from the plot in Fig. 5(a), where reference is made to a sample that underwent a short ageing period of 1 week. As the fatigue cycles proceed, a progressive decrease of the hysteresis energy occurs, as indicated in Fig. 5(c). The energy trend is interpolated by an exponential function and a 30% reduction is observed after 3000 cycles.

Different procedures can be adopted to perform thermo-mechanical tests aiming to evaluate the fatigue life of a SMA sample. The tests whose results are plotted in Fig. 5 reach a maximum deformation of 5.5%, with a net deformation of about 4.0%. Alternatively, the last set of cycles can be performed up to a maximum deformation of 3.14%, with a net deformation of 2.5-3.0%. The industrial costs of more sophisticated thermo-mechanical treatments (including, for instance, a series of working cycles at 310°K and successive series at room temperature) suggest to perform a minimal training at 3.14%, and then to directly use the samples in the dampers, with an available strain of 2.5-3.0%.

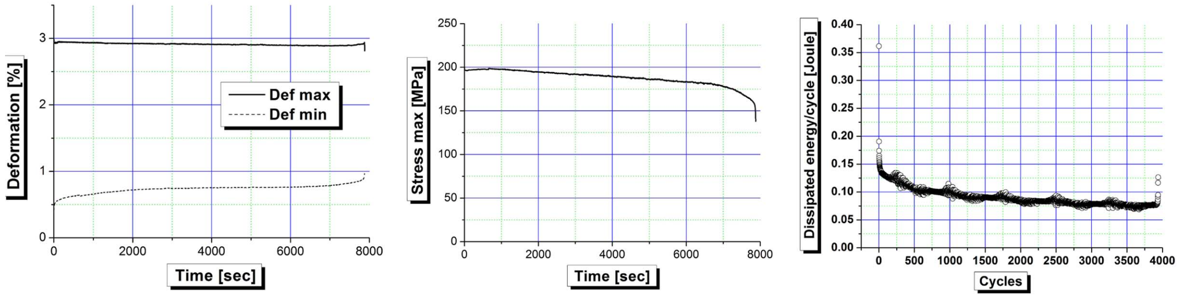

(a) (b) (c)

Fig. 6 Fatigue test, at 0.5 Hz, of a CuAlBe alloy with no initial training after a homogenization process of 10 min at 1023 K and the aging of 2 hours at 373 K. Cycles up to 3% of strain and down to zero load at a temperature of 323 K. Left: strain interval; Center: stress interval; Right: evolution of the dissipated energy in time

The results of a third test carried out in the laboratory of Pavia using an MTS 810 hydraulic machine equipped with a 25 kN actuator are shown in Fig. 6. They refer to a sample of CuAlBe alloy which was tested as furnished from the provider (the French company NIMESIS) without undergoing any initial training. The homogenization process is very short and it consists of 5 minutes at 1023 K, immediate water quench at room temperature, and finally 2 hours of aging at 373 K. The loading up to 3% of strain in span control is followed by an unloading in force-control with a frequency of one cycle every two seconds (0.5 Hz). The plot in Fig. 6(a) provides evidence of the creep phenomenon as the minimum deformation increases. The first cycle up to 3% of strain produces a permanent deformation of 0.5%. From the plot in Fig. 6(b) it can be observed a progressive deterioration of the alloy after an initial increase of the maximum stress. In Fig. 6(c), it is shown that the combination of the two observed phenomena results into a decrease of the energy dissipated along each cycle as the fatigue test proceeds.

Moreover, experiments were conducted using an MTS 810 hydraulic machine with a 100 kN actuator to investigate the dependency of the fatigue-life of CuAlBe alloys on stress and strain (true strain, i.e., the strain without the creep). Once again, the tests were carried out in two different laboratories: Bariloche, in Argentina, under the supervision of the last author, and Barcelona, Spain. Samples characterized by different durations of their homogenization process were tested. The results in Fig. 7 show that 1000 working cycles can be easily achieved using a homogenization process of 10 minutes at 1093 K, followed by an immediate quench in water at 293°K and a subsequent aging at 373 K. The measurements show that a satisfactory fatigue life (over 1000 working cycles) is clearly obtained for a net deformation up to 3%. The longest homogenization process, of duration 40 minutes, was performed at 1123 K on samples of significant length (about 1000 mm as required in damper devices), and it produced more brittle samples which showed an earlier failure.

4. Time constants

As underlined in the previous Sections, two direct effects of the "room" or aging temperature can be established. The first one is a slow effect that produces a change in the transformation temperature (whose value tracks the external aging temperature) and it is related to the diffusion effects on the

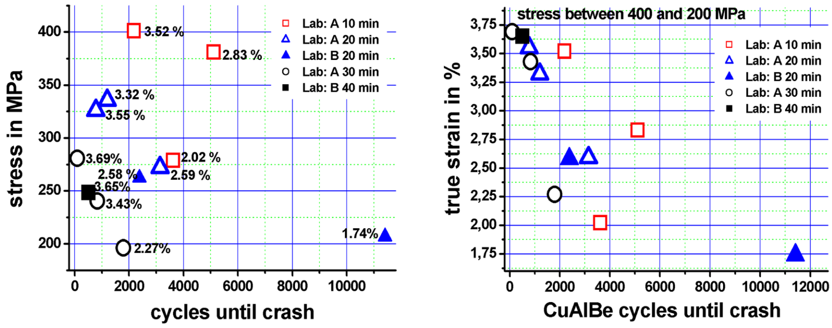

Fig. 7 Results from fatigue tests on CuAlBe wires of diameter 3.4 mm carried out at room temperature (293°K) and characterized by different heat treatments. The cycling frequency was set at 0.5 Hz. Left: plot of the maximum stress against the number of cycles to failure for five different durations of the homogenization treatments (10, 20, 30 and 40 minutes); the corresponding value of true strain is given in percentage. Right: plot of the associated true strain versus the number of cycles to failure. The strain values represent the true strain, having subtracted from the total strain the cumulative permanent deformation or SMA creep. The tests were carried out in two laboratories: A – Barcelona, Spain, and B – Bariloche, Argentina (Torra *et al*. 2009c)

atomic order. The second one is the immediate effect induced on the phase transition by the Clausius-Clapeyron thermodynamic equation. The hysteresis cycle rises to a higher stress level as the external temperature increases.

Studying the evolution of M_s (i.e., the starting transformation temperature from austenite to martensite) with the aging, several time constants (τ_1, τ_2, τ_3, …) can be estimated from experimental data of good quality. For instance, after a step at a given aging temperature, M_s shows an exponential behavior. In the case of a CuAlZn alloy, two time constants, τ_1 and τ_2, can be determined (Lovey and Torra 1999). When the CuAlBe alloy is considered, the aging induces a slower evolution than in the CuZnAl alloy and only one time constant can be determined. The time constant, τ_1, can be expressed as a function of temperature by considering the activation energy (5740 in °K units). Indeed, the following empirical relationship (Torra *et al.* 2009c) applies:

$$\mathrm{Log_e}(\tau_1) = -3.472 + 5740/T \tag{5}$$

with T in °K and τ_1 in s. The estimates of their values from the measurements taken on samples of a CuAlBe alloy are reported in Table 1.

The alloy reaches a steady state when a change of the room or aging temperature, ΔT_{RT}, produces a consequent change in M_s such that: $\Delta M_s = 0.135\ \Delta T_{RT}$. At a room temperature of about 293 K, the tracking of T_{RT} by the M_s value is highly delayed by a large time constant nearly equal to four

Table 1 Diffusion phenomena and asymptotic temperature effects of the atomic order on the value of M_s for a CuAlBe alloy

Parameters	Values estimated for a CuAlBe alloy (Casciati *et al*. 2008)
τ_1 from measures	1.95 days at 373°K
τ_1 from measures	4.63 days at 353°K
τ_1 extrapolated	116 days at 293°K
Activation energy	5740 K
$100\Delta M_s/\Delta T_{RT}$	13.5

months (116 days). For a single summer-winter wave of temperature with an amplitude of 10 K (that is, a variation of 20 K from peak to peak), the oscillation in the transformation temperature M_s is not larger than 1.4 K (or 3 K when measured from peak to peak).

The results indicate that the CuAlBe is appropriate for dampers allocated inside a building, where they are reasonably isolated from the external changes in temperature. In these conditions, the device temperature remains in the range from 278 to 308 K. The effect of a temperature change of 20 or 30 K during the summer-winter temperature cycles does not modify the transformation temperature by more than a wave in a peak to peak range between 2 and 4 K. The effect produced by the atomic diffusion changing the atomic order (which indirectly results in a stress increase of about 8 MPa in a CuAlBe alloy) is almost irrelevant when compared to the stress changes directly induced by the temperature wave due to the action of the Clausius-Clapeyron coefficient. For instance, a change of 30 K in the external temperature induces (at a rate of 2.2 MPa/K) an increase greater than 60 MPa in the position of the hysteresis cycles.

For a time duration of 20 or 30 years, the effect of a temperature change of 20 or 30 K during the summer-winter temperature cycles does not modify the transformation temperature by more than a wave in a peak to peak range between 2 and 4 K. Furthermore, the values of the time constants in Table 1 indicate that the action of daily temperature changes cannot produce significant evolution in the SMA material.

5. Family house application

A case study is identified within the class of structures to which the present application is targeted. The data from the laboratory tests are used to determine a numerical model that can take into account the effects of the SMA devices on the structural response to seismic excitation. The numerical results are validated by an experimental campaign conducted on a physical model mounting the actual devices.

5.1 The investigated portico

The rendering of a family house selected as case study is shown in Fig. 8. The structure is made by steel elements with concrete plates at the ground level (foundation), the first floor, and the roof level. The attention is focused on the bracing system of the portico located in the central part of the ground floor, underneath the first floor garden. A schematic representation of its geometrical details

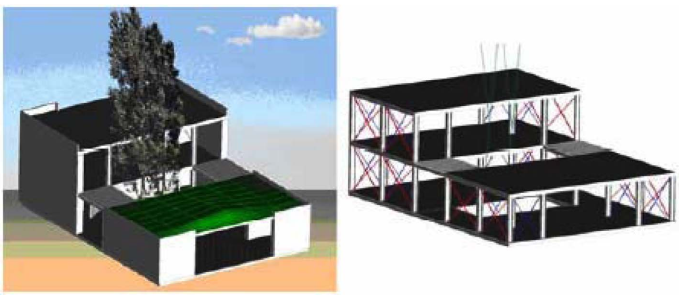

Fig. 8 Left: rendering of a family house with an inside garden, Right: placement of the SMA devices in the braces of the porticos (Torra *et al*. 2007b)

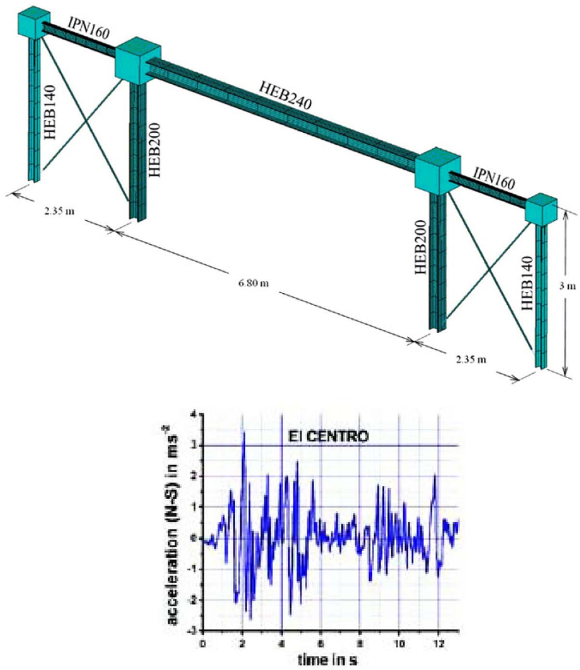

Fig. 9 Top: schematic view of the studied portico. The braces on the lateral porticos mount the devices made of SMA components, Bottom: segment of the "El Centro" accelerogram adopted as excitation (direction: N-S)

and static loading conditions is given in Fig. 9.

Each damper consists of CuAlBe wires of diameter 3.4 mm and it can be installed on the structure using the devices shown in Fig. 10(a). Its design in terms of length and number of the wires is driven by the following two considerations: 1) the wished portico oscillation must be a small percentage of the wire length; 2) the number of wires is computed in such a way that the global brace force is shared by the parallel wires consistently with the alloy constitutive law. A numerical simulation using 25 parallel wires of length 600 mm each was originally developed in (Torra *et al.* 2007b) and its main results are summarized in the next sub-section. Successively, a full scale test on a physical model of the portico mounting 2 wires of mean length 750 mm, (Fig. 10(b)) was carried out at UPC Barcelona and the results are reported in the last sub-section for the first time.

5.2 Numerical simulations

The response of the portico to the dynamic excitation induced by a segment of the "El Centro" accelerogram (which is shown at the bottom of Fig. 9) is evaluated by running the finite-element general-purpose code ANSYS. The two structural configurations with and without SMA dampers are considered.

A proprietary routine is introduced in the ANSYS software in order to simulate the SMA behavior. Basically, a bilinear model calibrated to be fully consistent with the indications arose from the laboratory tests is used Consistently with reference (Torra *et al.* 2007b), the adjective "bilinear" is herein adopted to denote that a loading or an unloading branch proceeds with a stiff linear

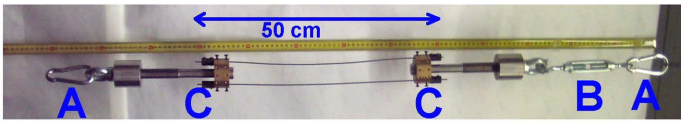

(a)

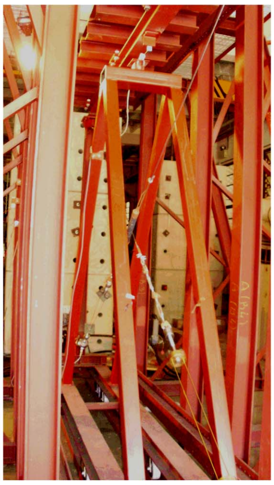

(b)

Fig. 10 (a) Details of a damper using two SMA wires of length 50 cm:. A: clamps; B: adjusting or pre-stressing device; C: hollow elements for the SMA wires connection. The compression in the SMA wires during the working cycles is avoided by enabling them to slip along the steel axis and (b) Picture of the CuAlBe SMA dampers mounted along the diagonals of the portico physical model. In the upper part of the inverted V-shape system, an HBM-LVDT sensor monitors the relative position of the portico beam versus time

segment followed by a soft linear segment. This explanation is given to avoid any confusion with the bilinear models used in plasticity. It is possible to improve the chosen phenomenological model to carefully describe all the minor internal loops of the hysteresis by using a fit of 8 bilinear models (Torra *et al.* 2007b), but for the present application the use of a bilinear model is satisfactory. Presently, a routine using cubic interpolations is under development to enable, a better fitting of the experimental results.

The portico was designed to rely on SMA braces and to survive the excitation with all the steel beams remaining in the elastic range for relevant deformations. The results of the simulation carried out on the portico without devices are presented in the form of displacements time history and they are reported on the left hand side of Fig. 11. In this case, a part of the steel pillars undergo plastic deformation, thus, inducing a permanently deformed shape of the frame at the end of the excitation. The simulation reported on the right hand side of Fig. 11 refers to the structure mounting SMA devices as braces in the lateral frames. Each device is modeled as 25 wires of CuAlBe alloy with a diameter of 3.4 mm each and a length of 60 cm. Steel cables are introduced to cover the remaining length of the portico diagonals. The modeled devices are not so stiff to prevent the portico from any motion, and they are able to avoid any residual deformation in fulfillment of the re-centering requirement. This performance is achieved by maintaining the steel beams in the elastic range and thanks to the super-elastic nature of the SMA constitutive law.

From the simulation results reported on the right hand side of Fig. 9, one can conclude that, when

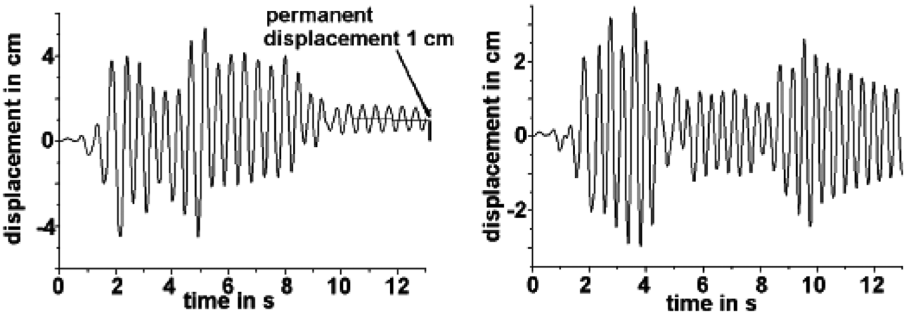

Fig. 11 Oscillations of the portico under the effects of the segment of the 'El Centro' accelerogram shown in Fig. 9(b). Left: without SMA devices, Right: with installed SMA devices, with no pre-stress

the dampers are "installed" without any pre-stress, the oscillation amplitude is nearly halved and no residual deformation is observed. The device effectiveness can be enhanced by pre-stressing the alloy bars. However, a permanent pre-stress in the Cu-based SMA should be avoided because it induces the martensite stabilization. Alternatively, an auto-pre-stress can be initiated during the quake by an appropriate mechanical device (see, for instance reference (Terriault *et al*. 2007)).

In conclusion, the simulation results indicate that the damping devices mounting CuAlBe SMA components can offer a very good performance if the SMA components work as they are expected. An appropriate selection of the number and the length of the SMA wires according to the intensity of the quake can halve the maximum amplitude.

5.3 Experimental campaign on a physical model of the portico

The experimental part of this study aims to demonstrate that, after an appropriate thermo-mechanical treatment, the CuAlBe components actually work as they are expected. In particular, the SMA elements are expected to show an appropriated fatigue life, not relevant creep effects, and not relevant consequences of the summer-winter temperature effects during several decades, if they are mounted inside the building. To verify these expectations, a test where the proposed devices could be actually installed on a real structure was set-up by the research team in Barcelona.

The physical model in Fig. 10(b) resembling a single portal of the portico is built over a ten-wheels trolley which moves along two U-shaped guidelines when activated by a hydraulic piston. The portico frame is made of HEB elements. In particular, it is formed by two pillars of length 2.47 m and an H cross-section 100×100 mm supporting an H beam of length 4.10 m and cross-section 120×120 mm. On top of the horizontal member, there is a series of short transverse elements which enables the placement of up to 4 masses in order to take into account the influence of the vertical loads. The frame is surrounded by a supplementary structure to avoid any out of plane oscillation. During actuation, the relative displacements of the portico beam are measured by an HBM linear variable differential transformer (LVDT) mounted on top of a fixed element inside the trolley. For this application, the damping devices consist of two wires of CuAlBe alloy placed in central position along each of the diagonals of the steel frame. Since the length of the SMA wires is shorter than the portico diagonals, steel cables are added at the edges to complete the braces by covering their full length.

During the experiments, two sets of measurements were taken. The first set refers to the portico

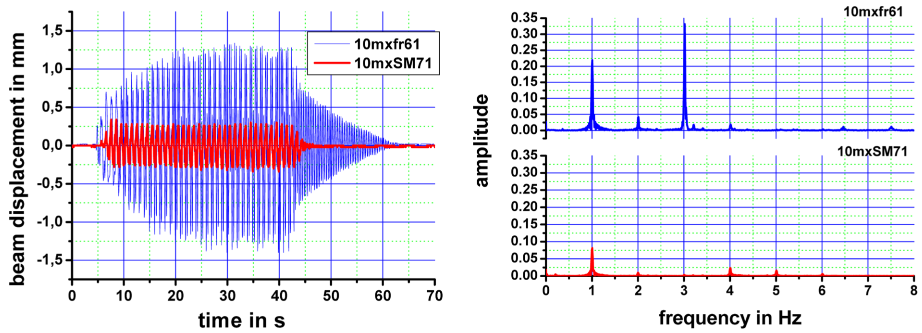

Fig. 12 Experimental results under an excitation frequency of 1 Hz and a peak to peak amplitude of 10 mm. The supplementary (vertical) load is zero. Left: free oscillation with (red) and without dampers (blue). Right: fourier transform of the beam displacements. Up: without SMA. Bottom: with SMA wire initially tensioned at 1.13 kN

without braces and it is graphically represented by the curves drawn in blue in Figs. 12 and 13. The second set is represented by the red curves in Figs. 12 and 13 and it characterizes the response of the portico braced with the SMA devices. From the comparison of the two sets of measurements, it is evident that the adoption of SMA braces leads to a drastic reduction of the oscillation amplitudes.

The results reported in Fig. 12 refer to an experiment where no vertical loads are added, the actuator produces sinusoidal oscillations of amplitude ± 5 mm at a frequency of 1 Hz, and the SMA wires are provided with a light pre-stress of 1.13 kN (i.e., 76 MPa; its location in the stress-strain diagram can be identified in Fig. 2). For this low excitation level, the use of SMA devices drastically reduces the oscillation amplitudes of the portico beam. In this case, the deformation and its associated stress do not exceed the levels required to induce the phase transition in the SMA wires. In fact, the analysis shows that almost no mechanical energy is transformed into heat. The SMA dampers work as simple “braces” at low stress (of about 1.2 kN) and the portico beam oscillations are almost entirely suppressed.

In the test of Fig. 13, four boxes of mass 1400 kg are added on the top of the portico beam and the actuator produces sinusoidal oscillations of amplitude ± 15 mm at a frequency of 1 Hz. The beam of the portico undergoes larger oscillations of amplitude ± 10 mm in comparison with the previous experiment, where oscillations of amplitude ± 1.3 mm were observed. Nevertheless, the introduction of SMA elements with a pre-stress force of 1.38 kN still enables a large reduction of the oscillations amplitude, which is decreased of about the 40% as shown on the left hand side of Fig. 13. Actually, the diagonal forces induce transformation in the SMA components and they cause the expected transfer of mechanical energy to heat in the SMA wires with the result that oscillation in the portico is nearly halved.

Without SMA, the Fourier transform of the beam displacements shows peaks at 1.0, 1.7 and 2 Hz (top right of Fig. 13). As expected, the increased load on the portico results in reduced frequencies' values. When the device mounting two SMA wires is introduced, the frequency spectrum is significantly modified (bottom right of Fig. 13). In this case, the absorbed energy transformed into heat is equal to 121 J. In the case of Fig. 12, for the reasons explained above, this energy was null. It is worth noting that, entering Fig. 4(c) with the test results, one only covers 60-80 cycles: therefore, in such an application, the martensite stabilization does not alter the response as the test proceeds from any starting point.

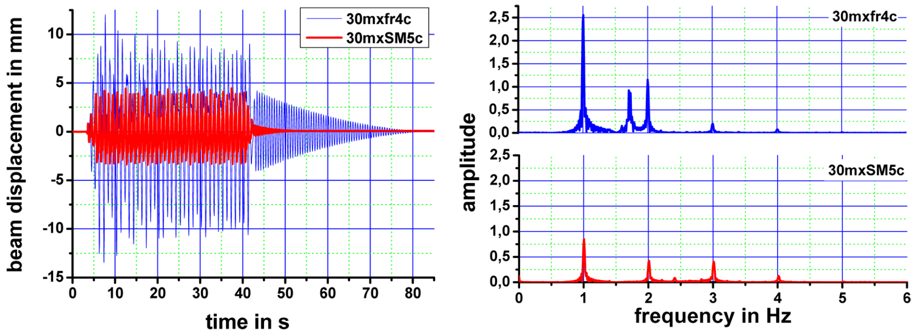

Fig. 13 Experimental results under an excitation frequency of 1 Hz and a peak to peak amplitude of 30 mm. The load on the upper part of the portico beam is due to a mass of 1400 kg. Left: free oscillation without (blue) and with dampers (red). Right: fourier transform of the beam displacements. Up: without SMA, Bottom: with SMA

In summary, the following comments can be addressed to the designers of brace devices in CuAlBe alloy:

1) a single shock of 100-200 seconds is compatible with the fatigue process of the alloy;
2) the aging process must be planned consistently with the phenomenon shown in Fig. 3 and with the governing parameters given in Section 4;
3) the mechanical training helps in smoothing the "creep" effect (see Fig. 2), which could result in a wire unwished elongation;
4) the temperature effects of the winter-summer cycles are well dominated in this alloy thanks to the reversibility of the phenomenon in Fig. 3.

6. Conclusions

The use of SMA elements in passive devices can produce positive effects in mitigating the damage during earthquakes. Nevertheless, the main conclusion achieved by the ongoing research activity, whose present results are summarized in this paper, is that, rather than a general purpose numerical material model, one should adopt case-specific numerical models in the structural analyses. They should account for the temporal scale, the spatial scale, and the thermo-mechanical treatments of preparation of the alloy and they should provide consistency with the results of a suitable experimental campaigns.

The case study reported in this paper suggests that phenomenological simple models deduced from experimental data can lead to satisfactory results, if they take into account the Clausius-Clapeyron effect. This approach confirms how the role of experimental tests is fully decisive in the implementation of shape memory alloy devices for engineering applications .

Acknowledgements

This paper summarizes the results achieved under separate grants to UPC from "M. Fomento" grants 2003/22 and 22/06, and to the Italian Universities from the research athenaeum funds (FAR

2009 to Pavia and PRA 2008 to Catania). Nevertheless, most of the exchanges between the principal investigators were realized thanks to the SOCRATES program which links the departments in Barcelona and Pavia. The authors are grateful to Mr. Jordi Lafuente of "Lab. Construcció" in building C1 of ETSECCPB – UPC for his support in the portico measurements and Mr. Pablo Riquelme of CAB- Bariloche, Argentina for his support in CuAlBe measurements. Finally, the authors are grateful to the referees who offered them the chance to clarify several aspects and to improve the readability of the paper.

References

ABS Consulting Inc.(2007), http://www.absconsulting.com/resources/Catastrophe_Reports/NotoHantoEarthquake.pdf.

Aernoudt, E., Van Humbeeck, J., Delaey, L. and Van Moorleghem, M. (1989), "Copper-base shape memory alloys: alloys for tomorrow", in *Proceedings of the Comett Course: The Science and Technology of Shape Memory Alloys*, V. Torra, Ed., Univ. Illes Balears, p. 221.

Auricchio, F., Faravelli, L., Magonette, G. and Torra, V. (2001), *Shape Memory Alloys: Advances in Modelling and Applications*, CIMNE, Barcelona, Spain.

Cardone, D. and Dolce, M. (2009), "SMA-based tension control block for metallic tendons", *International Journal of Mechanical Sciences*, **51**, 159-165.

Casciati S. and Faravelli L. (2008), "Structural components in shape memory alloy for localized energy dissipation", *Computers & Structures*, **86**, 330-339.

Casciati, F. and Faravelli, L. (2009), "A passive control device with SMA components: from the prototype to the model", *Journal of Structural Control and Health Monitoring,* **16**, 7-8, 751-765.

Casciati, F. and van der Eijk, C. (2008), "Variability in mechanical properties and microstructure characterization of CuAlBe shape memory alloys for vibration mitigation", *Smart Structures and Systems*, **4**, 2, 123-122.

Casciati, F., Casciati, S. and Faravelli, L. (2007), "Fatigue characterization of a cu-based shape memory alloy", *Proceedings of the Estonian Academy of Sciences – Physics Mathematics*, **56**(2), 207-217.

Casciati, F., Faravelli, L., Isalgue, A., Martorell, F., Soul, H. and Torra, V. (2008), "SMA fatigue in civil engineering applications", *Proceedings CIMTEC08, A10*.

Casciati, S. and Faravelli, L. (2006), "Fatigue tests of a cu-based shape memory alloy", *Proceedings of the 4th World Conference on Structural Control & Monitoring,* San Diego, USA.

Casciati, S. and Marzi, A. (2010), "Experimental studies on the fatigue life of shape memory alloy bars", *Smart Structures and Systems,* **6**(1), 73-86.

Dunne, D., Morin, M., Gonzalez, C. and Guenin, G. (2004), "The effect of quenching treatment on the reversible martensitic transformation in CuAlBe alloys", *Materials Science and Engineering A* **378**, 257-262.

Isalgue, A., Fernandez, J., Torra, V. and Lovey, F.C. (2006), "Conditioning treatments of Cu-Al-Be shape memory alloys for dampers", *Materials Science and Engineering A* 438-440, 1085-1088.

Isalgue, A., Torra, V., Yawny, A. and Lovey, F.C. (2008), "Metastable effects on martensitic transformation in SMA, Part VI. The clausius–clapeyron relationship", *Journal of Thermal Analysis and Calorimetry*, **91**(3), 991-998.

Johnson, R., Padgett, J.E., Maragakis, M.E., DesRoches, R. and Saiidi, M.S. (2008), "Large scale testing of nitinol shape memory alloy devices for retrofitting of bridges", *Smart Material and. Structures*, **17**(3), doi: 10.1088/0964-1726/17/3/035018.

Lovey, F.C. and Torra, V. (1999), "Shape memory in cu-based alloys: phenomenological behavior at the mesoscale level and interaction of martensitic transformation with structural defects in Cu-Zn-Al", *Progress in Materials Science*, **44**(3), 189-289.

Terriault, P., Torra, V., Fischer, C., Brailovski, V. and Isalgue, A. (2007), "Superelastic shape memory alloy damper equipped with a passive adaptive pre-straining mechanism", *Ninth Canadian Conference on Earthquake Engineering, Ottawa, Ontario*, Canada.

Torra, V., Auguet, C., Isalgue, A., Lovey, F.C., Sepulveda, A., Soul, H. (2009a), "Metastable effects on martensitic transformation in SMA", Part VIII. Temperature Effects on Cycling, *J Therm. Anal. Calorim*., DOI

10.1007/s10973-009-0613-3.
Torra, V., Isalgue, A., Auguet, C., Carreras, G., Lovey, F.C., Soul H. and Terriault, P. (2009b), “Damping in civil engineering using SMA. The fatigue behavior and stability of CuAlBe and NiTi alloys”, *J. of Materials Engineering and Performance_ASM Internacional*, DOI: 10.1007/s11665-009-9442-6.
Torra, V., Isalgue, A., Auguet, C., Lovey, F., Pelegrina, J.L. and Terriault, P. (2007a), “Pre-stressed NiTi: effects of the thermodynamic forces and time”, *Proc. SMST*, Tsukuba.
Torra, V., Isalgue, A., Martorell, F., Casciati, F., Lovey, F.C., Peigney, M., Terriault, P., Tirelli, D. and Zapico, B. (2009c), “SMA in mitigation of extreme loads in civil engineering: damping of earthquake effects in family houses and in wind/rain perturbations on stayed cables in bridges”, Proc. PROTECT2009, Japan.
Torra, V., Isalgue, A., Martorell, F., Terriault, P. and Lovey, F.C. (2007b), “Built in dampers for family homes via SMA: An ANSYS computation scheme based on mesoscopic and microscopic experimental analyses”, *Engineering Structures* **29**, 1889-1902.
Wollants, P., Roos, J.R. and Delaey, L. (1993), “Thermally-induced and stress-induced thermoelastic martensitic transformations in the reference frame of equilibrium thermodynamics”, *Progr. Mater. Sci*., **37**(3), 227-288.

BS